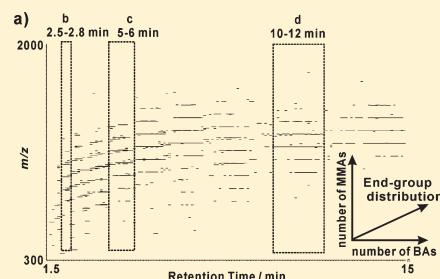


End-Group Analysis of Methacrylic (Co)polymers by LC-ESI-MS<sup>2</sup>Junkan Song,<sup>†</sup> Jan W. van Velde,<sup>†</sup> Luc L. T. Vertommen,<sup>†</sup> Donald F. Smith,<sup>‡</sup> Ron M. A. Heeren,<sup>‡</sup> and Oscar F. van den Brink<sup>\*,†</sup><sup>†</sup>Research, Development and Innovation, AkzoNobel, Deventer, The Netherlands<sup>‡</sup>FOM Institute for Atomic and Molecular Physics, Amsterdam, The Netherlands

Supporting Information

**ABSTRACT:** End-group analysis was achieved on poly(methyl methacrylate) and poly(methyl methacrylate-*r*-butyl acrylate) by liquid chromatography–electrospray ionization–ion trap mass spectrometry (LC-ESI-IT MS) and electrospray ionization–Fourier transform ion cyclotron resonance tandem mass spectrometry (ESI-FTICR MS<sup>2</sup>). The two polymers were produced by radical polymerization in butyl acetate at relatively high temperature using the same initiator, *tert*-butylperoxy-3,5,5-trimethylhexanoate. In both polymers, structures with different end-groups were successfully assigned using gradient elution LC-IT MS, with the aid of exact mass experiments in an FTICR MS instrument. Isobaric materials in PMMA were discriminated using accurate mass FTICR MS<sup>2</sup>. Isocratic LC-MS reduced the complexity of the data of P(MMA-*r*-BA), made the attribution of peaks easier, and shortened the experimental time compared to gradient elution LC-MS. The identification of end-groups in both the methacrylic homo- and copolymer demonstrated that  $\beta$ -scission and radical transfer to solvent play an important role in the polymerization.



## INTRODUCTION

The demand of copolymeric materials in daily life has been growing in the past decades. Many new copolymers have been developed to meet the consumer and industry needs.<sup>1–3</sup> A number of new polymerization techniques have been invented to serve the purpose of synthesizing polymers with more complicated and targeted structures. Controlled/living radical polymerization<sup>4</sup> such as stable free radical polymerization (SFRP),<sup>5</sup> atom transfer radical polymerization (ATRP),<sup>6</sup> and reversible addition–fragmentation chain transfer polymerization (RAFT)<sup>7</sup> are the best examples of the newly developed polymerization methods.

Among all polymerization methods, free radical polymerization is one of the very often used methods to synthesize polymers in industry. Peroxide initiation has been intensively studied using various methods in the past.<sup>8</sup> Three stages are involved in the polymerization: initiation, chain propagation, and chain termination. Transfer reactions may occur throughout the polymerization and contribute to all three stages. A detailed scheme of the initiation mechanism can be found elsewhere.<sup>9</sup> Basically, for the initiator Trigonox 42S used in this study, octyl radicals (C<sub>8</sub>H<sub>17</sub>•, *r*), and methyl radicals (CH<sub>3</sub>•, *m*) were produced to start the polymerization. Under the conditions applied, radical transfer to solvent or monomer can also occur and start the polymerization.<sup>9</sup> The many possibilities of initiation species will result in a variety of end-groups.

High-temperature (>120 °C) radical polymerization introduces some specific initiation and termination mechanisms. An intramolecular chain transfer reaction, namely intramolecular backbiting, observed in many cases,<sup>10–16</sup> will increase the complexity of the end-group distribution. The backbiting reaction

forms a tertiary carbon-centered radical by hydrogen abstraction to a secondary carbon at the chain end or a tertiary carbon on the main chain. The carbon-centered radical formed undergoes  $\beta$ -scission to generate a  $\beta$ -scission radical and a terminally unsaturated chain. The mechanism of  $\beta$ -scission of a poly(methyl methacrylate) (PMMA) chain is shown in Scheme 1. Two  $\beta$ -scission routes are possible that can happen on either side of the molecule and therefore generate four different structures. Route I will produce two molecules with identical structures as a normal propagating chain and a terminally unsaturated chain generated by disproportionation. Route II, on the other hand, will produce two molecules: one having a CH<sub>2</sub> group more in the backbone ( $\beta^1$ ) than from route I and the other having one CH<sub>2</sub> less in the backbone ( $\beta^2$ ). A similar mechanism on a poly(*n*-butyl acrylate) (PBA) chain was presented in a previous study.<sup>9</sup> As a consequence, four oligomers ( $\beta^{1a}$ ,  $\beta^{1b}$ ,  $\beta^{2a}$ , and  $\beta^{2b}$ ) will be generated through four pathways, which can be terminated in many different ways.

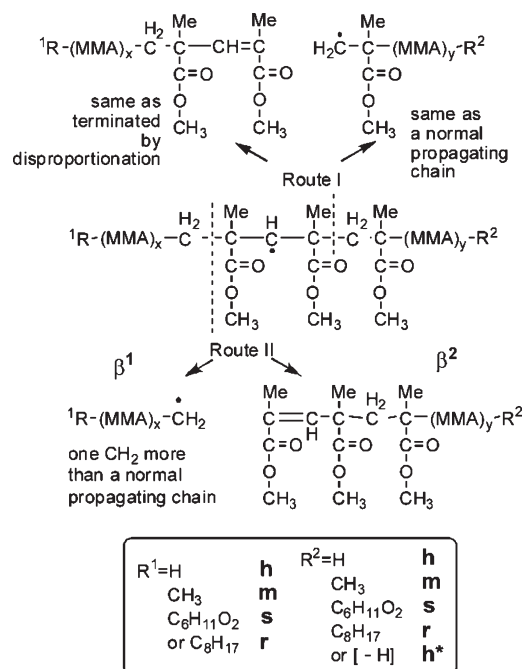
In addition, solvent effects in radical polymerization such as chain transfer to solvent have also been observed and investigated in several studies,<sup>17–19</sup> including our previous investigation of poly(*n*-butyl acrylate)s.<sup>9</sup> Our previous study clearly showed that the relatively reactive solvents used in the polymerization had a strong influence on the polymer composition under the conditions applied. It is the aim of this study to identify the end-groups of PMMA and P(MMA-*r*-BA) prepared under similar conditions, reflecting the polymerization mechanisms.

Received: November 25, 2010

Revised: January 18, 2011

Published: February 03, 2011

**Scheme 1.  $\beta$ -Scission of Methyl Methacrylate (MMA) Radical Polymerization in Butyl Acetate as Solvent under Relatively High Temperature<sup>a</sup>**



<sup>a</sup> h = hydrogen, m = methyl, s = solvent residue, r = radical residue, and h\* = unsaturated end-group resulting from disproportionation. For a further explanation of the nomenclature, see ref 9.

For the analysis of increasingly complicated polymer structures more potent techniques are required. Most polymeric materials have a molecular weight distribution, a functionality distribution such as different end-groups, and a composition distribution (in copolymer). Classic methods such as size exclusion chromatography (SEC) can be applied to determine the molecular weight distribution of polymers. Gradient elution of polymers has been developed to separate polymers according to their polarity (and can therefore be used for separation based on end-group and/or the heterogeneity of copolymer). Liquid chromatography at critical conditions of adsorption (LACCC) has also been studied and applied to many polymer systems.<sup>20–22</sup> Under the (near-)critical condition of adsorption, the elution of a polymer is independent of its molecular weight distribution but only based on its end-group functionality. This offers a possible solution to analyze a complicated copolymer system if the near-critical condition of a monomer fraction is achieved.

Electrospray ionization–mass spectrometry (ESI-MS)<sup>23,24</sup> alone is able to discriminate among different masses and has a remarkably high sensitivity. Furthermore, tandem MS can produce fragment ions for partial or complete structural determination.<sup>25,26</sup> The use of chromatography and MS techniques has proven to be mutually complementary and powerful for polymer structural analysis. Montaudo et al.<sup>27</sup> demonstrated use of SEC-MALDI MS measurement on a P(MMA–BA) copolymer system to determine the bivariate distribution. Gruendling et al.<sup>28</sup> demonstrated the application of SEC-ESI MS on the determination of absolute individual molecular weight distributions from polymer mixtures (same monomer class but different end-groups). The approach of LACCC-MS has been applied to poly(ethylene oxides), poly(propylene oxides), and their copolymers by several researchers.<sup>29,30</sup>

**Table 1. Molecular Weight Distribution of PMMA and P(MMA-*r*-BA) Obtained by GPC**

monomer	methyl methacrylate	methyl methacrylate and <i>n</i> -butyl acrylate
$M_n$ (g/mol)	3300	1600
$M_w$ (g/mol)	7300	3500

Some other attractive and recently developed methods, such as LC-NMR-MS<sup>31</sup> or IMS-MS,<sup>32,33</sup> will also offer information on end-group structures. Both techniques, however, have only had limited application in the characterization of synthetic polymers so far.

In this study, both gradient elution LC and isocratic elution LC are coupled to ESI-MS to investigate the structures of PMMA and P(MMA-*r*-BA). The variety of combined masses of the end-groups of a polymer observed by LC-IT MS is further investigated using high-resolution and high-accuracy FTICR MS/MS. By gradient elution LC, a separation based on polarity (end-group functionality) and molecular weight distribution is obtained for PMMA and its copolymer with BA. Isocratic elution is applied to reduce the effects of MMA on elution and therefore shortened the experimental time and reduced the complexity of the spectra.

## EXPERIMENTAL SECTION

**Polymer Synthesis.** All the samples analyzed in this study were supplied by AkzoNobel Car Refinishes, Sassenheim, The Netherlands. They were prepared by radical polymerization in butyl acetate as solvent under relatively high temperature (160 °C) using *tert*-butylperoxy-3,5,5-trimethylhexanoate [Trigonox 42S] as initiator. In both cases, the monomer-to-solvent ratio was 1:1.25 (w/w) and 5% initiator was used. Monomer and initiator were fed in a constant rate over 4 h. The ratio of monomers used in the copolymer sample was 1:1.

The molecular weight averages of samples were measured by GPC calibrated with poly(methyl methacrylate) standards on 2 × PLGel 5  $\mu$ m Mixed-D columns (300 mm × 7.5 mm) using THF as eluent at a flow rate of 1 mL/min. Refractive index detection was used. Table 1 lists the molecular weight averages obtained by GPC of the methyl methacrylate homopolymer and the methyl methacrylate–butyl acrylate copolymer.

**Mass Spectrometry.** Mass spectra were acquired by direct infusion electrospray ionization–mass spectrometry (ESI-MS) and liquid chromatography–ESI–MS (LC-ESI-MS). Two mass spectrometers, viz. a Thermo Scientific LTQ FT Ultra Hybrid and a Bruker Esquire 3000plus, were used in this study.

For analysis employing direct infusion (using a Cole-Parmer 74900 series syringe pump at 0.6 mL/h) samples were dissolved in methanol (Fluka) at an approximate concentration of 100  $\mu$ g/mL. The LTQ FT-ICR was externally calibrated with LTQ calibration mix (50% methanol in water; Sigma-Aldrich, Zwijndrecht, The Netherlands) and Automatic Gain Control (AGC)<sup>34</sup> was used. AGC ensures that the same number of ions is injected in the ICR cell for each scan, thus minimizing mass shifts due to changes in number of ions. The capillary voltage was set to 3.0 kV, capillary temperature to 275 °C, sheath gas flow rate to 4.94 units, and resolving power to 100 000.

For LC-MS analysis, samples with a concentration of 2 mg/mL in THF were prepared. The LC system was an Agilent 1100 series LC binary pump with DAD detector. The LC column in the LC-ESI-MS setup was an Alltech Kromasil C18 150 mm × 4.6 mm, 5  $\mu$ m (Deerfield, IL). During analysis, the column temperature was thermostated at 30 °C. A gradient of tetrahydrofuran (THF) (Sigma-Aldrich)/acetonitrile (ACN)

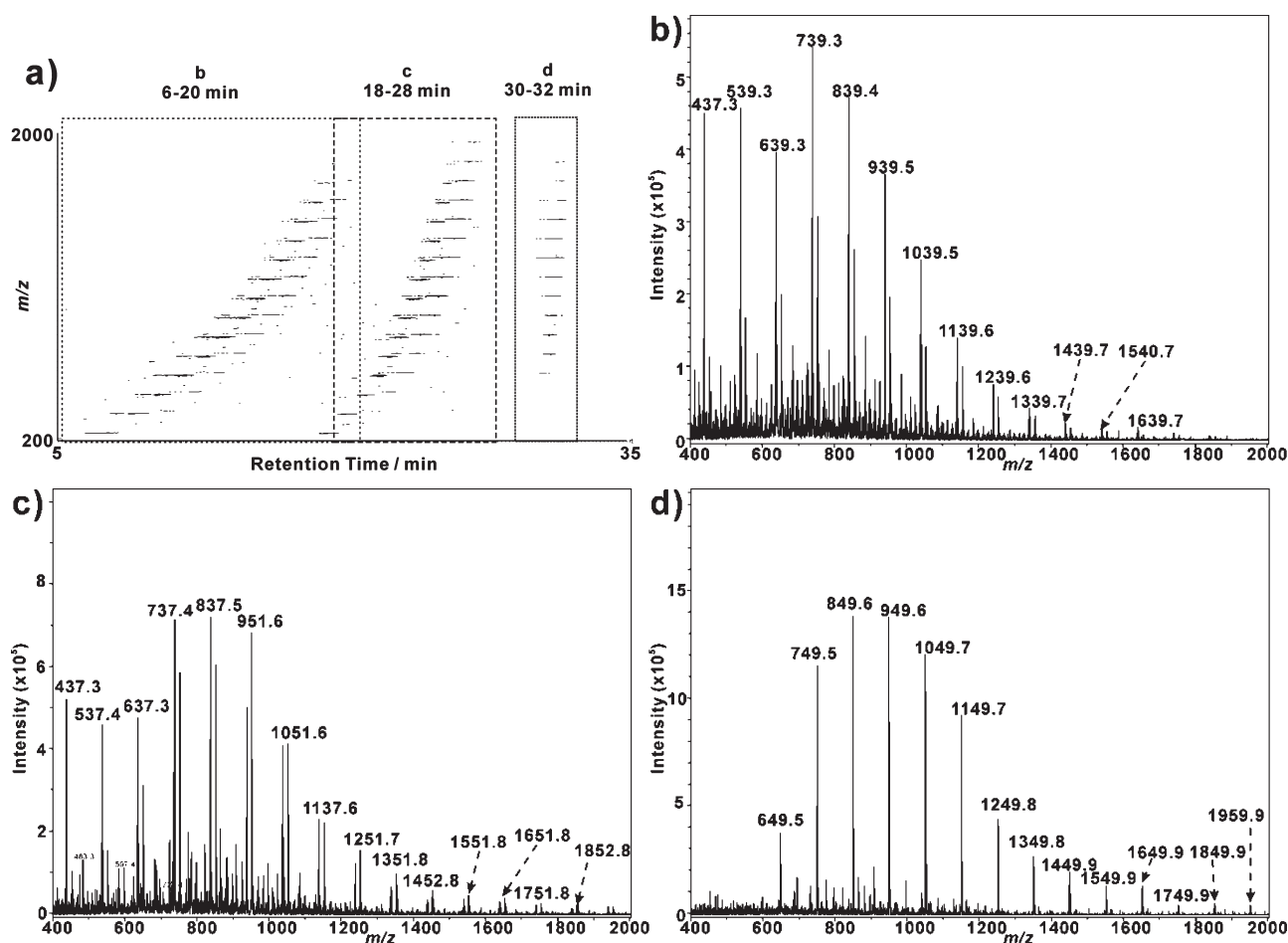


**Figure 1.** (a) Gradient elution LC-IT-MS data showing log abundance of the PMMA with sodium adduct ions (data point weight) in a coordinate system of  $m/z$  (as  $y$ -axis) versus retention time (as  $x$ -axis); PMMA is predominantly detected as singly charged adduct ions. The corresponding average mass spectra of PMMA in different range of retention time: b, 6–20 min; c, 18–28 min; d, 30–32 min.

(Sigma-Aldrich) and  $\text{H}_2\text{O}$  (from Millipore Direct-Q) (55:45 v/v, premixed) was used as mobile phase. Formic acid (FA) (Fluka) at a level of 0.1% was added to both mobile phases. The settings of the instrument, a Bruker Esquire 3000plus (Bruker, Germany), were the following: capillary voltage 3 kV; nebulizer pressure 60.0 psi; drying gas flow 11.0 L/min; drying gas temperature 360 °C; maximum accumulation time 50.0 ms.

Data were processed and analyzed using Thermo Scientific Excalibur 2.0 and Bruker DataAnalysis 3.3 data systems, respectively.

## RESULTS AND DISCUSSION

**Gradient Elution LC-MS of PMMA.** LC separation was used prior to and online with MS. A wide range of gradients was tested to optimize the LC separation. The best separation of the PMMA samples was achieved using a gradient from 5% THF/95% ACN and  $\text{H}_2\text{O}$  (55:45 v/v, premixed) to 100% THF in 60 min. The selection of mobile phase is based on the solubility of PMMA in these solvents. In this gradient setting, THF is a strong solvent for PMMA, ACN is a poor solvent for PMMA, and  $\text{H}_2\text{O}$  is a nonsolvent.<sup>35</sup> All oligomers were detected as sodium adduct ions,  $[\text{M} + \text{Na}]^+$ , presumably formed as a consequence of the presence of residual sodium salts in the solvents. Multiply charged peaks were observed with very low intensity and therefore not taken into consideration in this study.

Figure 1a shows the partial (retention time 2–35 min) LC-MS data showing log abundance of the PMMA(A) molecules with

sodium adduct ions (data point weight) as  $m/z$  (as  $y$ -axis) versus chromatographic elution time (as  $x$ -axis). Clear distributions of the peaks with  $m/z$  differences of 100 (singly charged) along the  $y$ -axis are attributed to the mass of MMA (100 Da). The distributions along the retention time ( $x$ -axis) originate from PMMA with various end-groups and molecular weight distributions. The corresponding average mass spectra of the three ranges of retention time are shown in Figure 1: b, 6–20 min; c, 18–28 min; d, 30–32 min.

According to the gradient elution conditions used, structures with higher polarity and lower molecular weight will elute earlier in the LC. The  $\alpha$ -end-groups potentially present in this PMMA sample include hydrogen (H), methyl ( $\text{CH}_3$ ), and octyl ( $\text{C}_8\text{H}_{17}$ ) from the initiator and residue ( $\text{C}_6\text{H}_{11}\text{O}_2$ ) from the solvent (butyl acetate). Unsaturated end-groups are also possible due to  $\beta$ -scission (see Scheme 1) and disproportionation. Among all, structures with either H or  $\text{CH}_3$  end-group will have a higher polarity than those with  $\text{C}_8\text{H}_{17}$  as end-group. In line with this reasoning, three elution time windows are observed: PMMA with no  $\text{C}_8\text{H}_{17}$  end-group (6–20 min; Figure 1b), with  $\text{C}_8\text{H}_{17}$  end-group at one end of the polymer chain (18–28 min; Figure 1c), and with  $\text{C}_8\text{H}_{17}$  end-group at both ends of the polymer chain (30–32 min; Figure 1d).

Because ITMS does not allow confirmation of the elemental composition of the end-groups due to lack of mass accuracy,



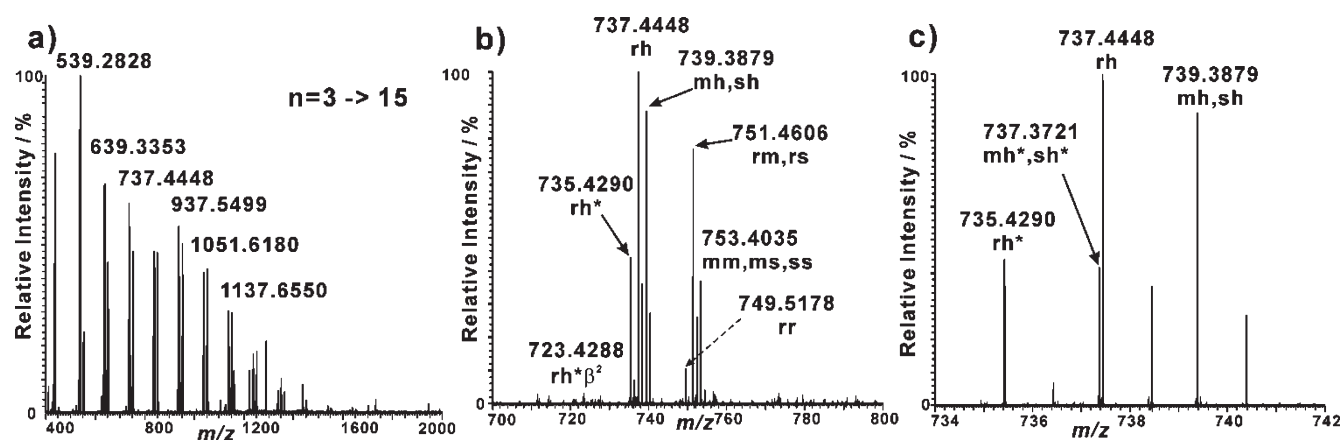


**Figure 2.** Average mass spectra of PMMA obtained by FTICR-MS summed over 2 min: (a) the entire scan range  $m/z$  400–2000, (b) expanded ( $m/z$  700–800) mass spectra with series assignment, (c) further expanded ( $m/z$  734–742) mass spectra with series assignment.

the homopolymer sample was analyzed by FT-ICR-MS. Figure 2 shows the summation spectra of ESI-FTICR MS data of PMMA.

Although LC was not applied prior to the experiment and hence the polymer sample was not separated in time based on end-group, the resolution and mass accuracy of the FTICR MS instrument were sufficient to discriminate and identify the majority of the peaks. Although some of the peaks have relatively lower intensity in the FTICR MS spectra than in the IT MS spectra (they might have suffered from ion suppression in the infusion experiment), the infusion FTICR MS data are still qualitatively valid for structure elucidation. Using linear regression,<sup>36</sup> exact residual masses of every series resulting from the various initiation and termination mechanisms were obtained. The naming system used in Figure 2 is similar to that used in previous reports.<sup>8,9</sup> For example, series  $rh^*$  with  $m/z$   $335 + 100(n - 3)$  was attributed to the structures resulting from initiation by octyl radical from the peroxide initiator and termination by disproportionation to form an unsaturated end-group. The calculated residual mass for the series was 139.1144 Da, which is exactly the theoretical mass of  $[C_8H_{16} + Na]^+$ . The standard deviation of the data is 1 ppm. The theoretical exact mass of an MMA monomer is 100.0524 Da while the calculated value is also exactly  $100.0524 \pm 0.0001$  Da. A more detailed description of procedure of the method can be found in the Supporting Information. This example shows that the unequaled high accuracy and resolution of FTICR MS instrument makes it a very powerful and suitable tool to determine the exact masses and corresponding elemental compositions in complex synthetic polymer systems.

In the LC-IT MS data, the series  $m/z$   $337 + 100(n - 2)$  (nominal mass) was observed in both the retention time window 6–20 min and the retention time window 18–28 min. The results obtained by FTICR MS reveal the existence of isobaric materials at these nominal masses. In Figure 2c, split peaks were observed at  $m/z$  737.3721 and  $m/z$  737.4448, with a 0.0727 Da mass difference. The elemental compositions are  $C_{36}H_{58}O_{14}$  and  $C_{38}H_{66}O_{12}$ , calculated from the exact mass data. The end-groups are assigned as  $C_6H_{10}O_2$  and  $C_8H_{18}$ , respectively. The two peaks were therefore attributed to series  $sh^*$  (or  $mh^*$ ) and  $rh$ . The theoretical mass difference of these two structures is 0.0728 Da ( $\Delta < 0.0001$  Da). FTICR MS<sup>2</sup> further supports this attribution since different fragmentation pathways were observed. By applying a broad isolation window, both  $m/z$  737.3721 and  $m/z$  737.4448 were selected as precursor ions so that product ions

were produced from both structures. On the other hand, application of a narrower isolation window to only include the more intense peak  $m/z$  737.4448 as precursor ion was applied to generate product ions only from this structure. The product ions exclusively observed when a broad excitation window was applied could therefore be assigned to be the fragments from the peak observed at  $m/z$  737.3721. Figure 3 shows FTICR MS<sup>2</sup> spectra of  $m/z$  737.4 obtained at different isolation windows. Figure 3a was obtained using the relatively broad isolation window ( $m/z \pm 0.2$ ), and Figure 3b was obtained using the very narrow isolation window ( $m/z \pm 0.05$ ). Thus, only  $m/z$  737.4448 was selected as precursor ion in Figure 3b. Losses of 100.0524 (from loss of a monomer unit of MMA) were observed in both cases. In Figure 3a two peaks with comparable intensity at  $m/z$  637.3195 and  $m/z$  637.3924 were detected (calculated from  $m/z$  737.3721 and  $m/z$  737.4448, respectively). In Figure 3b an intense peak is observed at  $m/z$  637.3924 (originating from  $m/z$  737.4448). A very minor peak present at  $m/z$  637.3195 confirms that little  $m/z$  737.3721 was selected as precursor ion in this case and that the difference between parent and product ions agrees with the elemental composition of MMA ( $C_5H_8O_2$ , theoretical exact mass 100.0524 Da). A unique loss of  $m/z$  60.0211 was only observed in the MS<sup>2</sup> spectra including  $m/z$  737.3721 as precursor ion. The loss is attributed to acetic acid ( $C_2H_4O_2$ ) from the end of the polymer chain (resulting from the initiation by the butyl acetate solvent radical).<sup>9</sup> It agrees well with the theoretical mass of  $C_2H_4O_2$ , which is exactly 60.0211. Nominally isobaric peaks were observed up to  $m/z$  1437 (resolution is 19 700). Larger molecules were not well ionized in the infusion FTICR experiment and produced peaks with low intensities. A possible cause of this is the use of methanol but not THF as the solvent. Unfortunately, the experimental setup did not allow the use of THF, so no experiment could be carried out in this solvent.

**Gradient Elution LC-MS of P(MMA-*r*-BA).** The same gradient used for LC-MS experiment of PMMA was applied to study P(MMA-*r*-BA). Figure 4a is the partial (retention time 2–40 min) gradient elution LC-MS data obtained by IT MS showing log abundance of the P(MMA-*r*-BA) with sodium adduct ions (data point weight) in a coordinate system of  $m/z$  (as  $y$ -axis) versus retention time (as  $x$ -axis). The average mass spectrum of P(MMA-*r*-BA) obtained by gradient elution LC-IT MS is shown in Figure 4b, and Figure 4c shows the average mass spectrum of P(MMA-*r*-BA) obtained by FTICR MS without preceding LC separation.

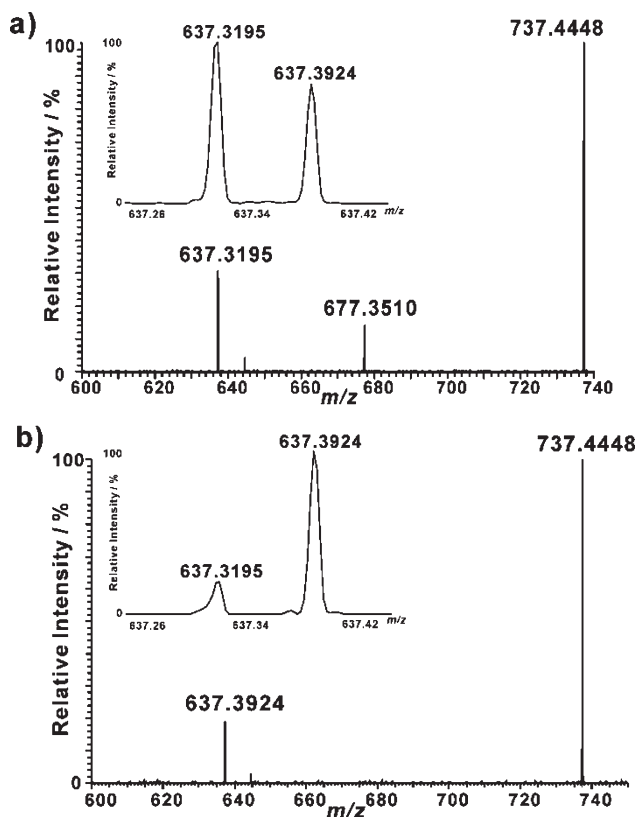


**Figure 3.** FTICR MS<sup>2</sup> spectra (summed over 2 min) of  $m/z$  737.4: (a) isolation window  $m/z \pm 0.2$ ; (b) isolation window  $m/z \pm 0.05$ . Insets are the corresponding expanded MS<sup>2</sup> spectra ranging from  $m/z$  637.24 to  $m/z$  637.42.

The LC-MS data set of the copolymer system, as expected, is more complicated than the homopolymer system due to the addition of the BA fraction. Structures with different end-groups, however, can still be discerned and attributed. The FTICR MS data aided calculation of elemental compositions and thus facilitated further end-group structure assignment. Table 2 lists all observed series assignments (end-group combinations) with their retention time range and corresponding masses. Interestingly,  $\beta$ -scission is involved in almost all dominant end-group combinations. The cause of this is the relatively high polymerization temperature and the corresponding high probability of  $\beta$ -scission reaction for both monomers.

The FTICR MS spectra are less complicated than the LC-IT MS spectra. Several series were not observed in the FTICR MS spectra. The possible cause of this observation is again the initial solvent used for the experiments in the infusion analysis. Some polymer structures might have very low solubility in methanol. Another possible cause is the ion suppression effects in the infusion experiment. The combination of LC separation and summation over the separated peaks, however, mitigated and decreased this effect and gives a better reflection of the composition of the sample.

**Isocratic Elution LC-MS of PMMA and P(MMA-*r*-BA).** Isocratic elution LC-MS was applied to both PMMA and P(MMA-*r*-BA) samples. The mobile phase used was 50% THF/50% ACN and H<sub>2</sub>O (55:45 v/v, premixed). This is similar to the condition used in earlier research done by Cools et al.<sup>37</sup> and Philipsen et al.<sup>38</sup> The aim of applying this isocratic condition is to achieve a near-critical separation on PMMA and to expand the study of

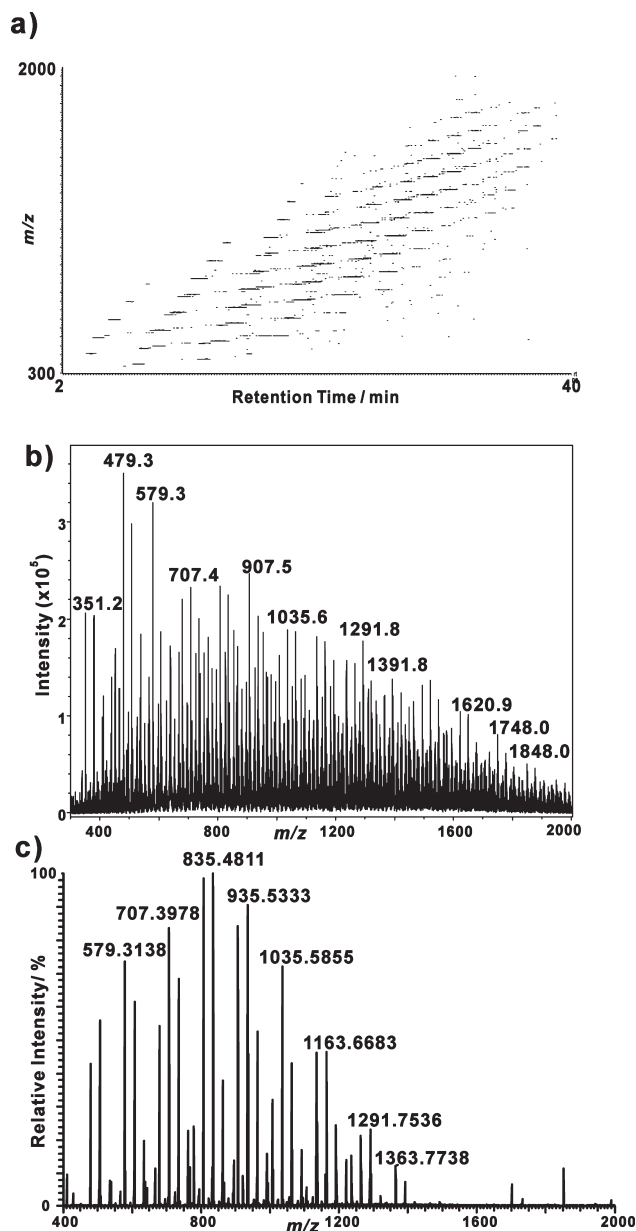


**Figure 4.** (a) Gradient elution LC-IT-MS data showing log abundance of the P(MMA-*r*-BA) with sodium adduct ions (data point weight) in a coordinate system of  $m/z$  (as y-axis) versus retention time (as x-axis), (b) average mass spectrum of P(MMA-*r*-BA) obtained on gradient elution LC-IT MS (summation range: 2–40 min,  $m/z$  300–2000), and (c) average mass spectrum of P(MMA-*r*-BA) obtained by FTICR MS ( $m/z$  400–2000).

**Table 2.** P(MMA-*r*-BA) Series with Corresponding Elution Time in Two Elution Conditions<sup>a</sup>

gradient elution time (min)	0–18	8–31.5	30–40
isocratic elution time (min)	0–2.5	2.4–7.6	7.5–15
series assignment <sup>b</sup>	$\beta^{1a}_s$	$\beta^{1b}_s$ or $\beta^{2a}_s$	$\beta^{2a}_r$
residual mass	39, 67, 95	51, 79, 07, 35, 63, 91, 19, 47	33, 61, 89, 17, 45

<sup>a</sup> Observed range of number of MMA is 0–18 and number of BA is 0–14. <sup>b</sup> See Supporting Information for the end-group structure illustration.

P(MMA-*r*-BA). Generally, in an AB copolymer system, if critical condition is achieved on A, the elution will not be affected by A but only by B and the total end-group functionality.

Figure 5 shows the isocratic elution LC-MS data obtained on IT MS as log abundance of the PMMA with sodium adduct ions (data point weight) in a coordinate system of  $m/z$  (as  $y$ -axis) versus retention time (as  $x$ -axis).

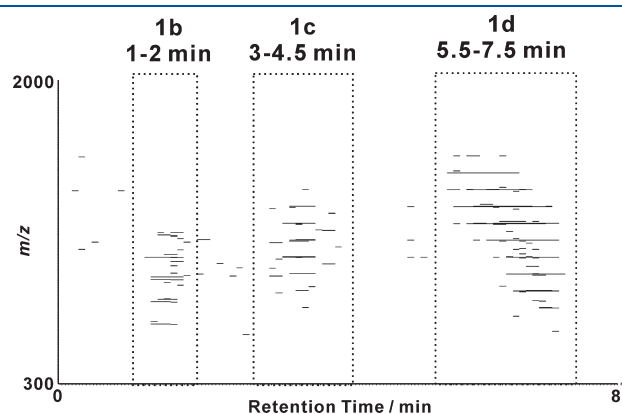


**Figure 5.** Isocratic elution LC-MS data obtained on IT MS showing log abundance of the PMMA with sodium adduct ions (data point weight) in a coordinate system of  $m/z$  (as  $y$ -axis) versus retention time (as  $x$ -axis).

Three elution time windows were observed in the data. They correspond to the three areas observed in Figure 1b–d. PMMA with the same end-group functionality eluted in the same elution time window despite its molecular weight distribution. The axes of Figure 5 can therefore be transformed to end-group functionality or number of octyl end-groups ( $x$ -axis) and molecular weight or degree of MMA polymerization ( $y$ -axis).

Figure 6a shows the isocratic elution LC-MS data obtained on the copolymer using IT MS and plots log abundance of the P(MMA-*r*-BA) with sodium adduct ions (data point weight) in the coordinate system of  $m/z$  (as  $y$ -axis) versus retention time (as  $x$ -axis). The corresponding average mass spectra of P(MMA-*r*-BA) in different retention time windows are shown in Figures 6b (2.5–2.8 min), 6c (5–6 min), and 6d (10–12 min).

Major peaks in the mass spectrum shown in Figure 6b all have the same end-groups and number of BA units (2) but a different number of MMA units. The structures are attributed to series  $\beta^{1a}$ s, which results from a solvent radical initiation chain that underwent  $\beta$ -scission and was terminated by hydrogen abstraction. Likewise, in Figures 6c and 6d, all the peaks have the same end-groups (series  $\beta^{1b}$  or  $\beta^{2a}$ s for Figure 6c and series  $\beta^{2a}$ r for Figure 6d) and number of BA units (both 5 for Figure 6c and Figure 6d) but different numbers of MMA units. Thus, between each consecutive pair of retention time windows, the residual masses differed by 28 Da (viz. the substitution of one MMA with one BA). The results confirmed this elution condition is based on

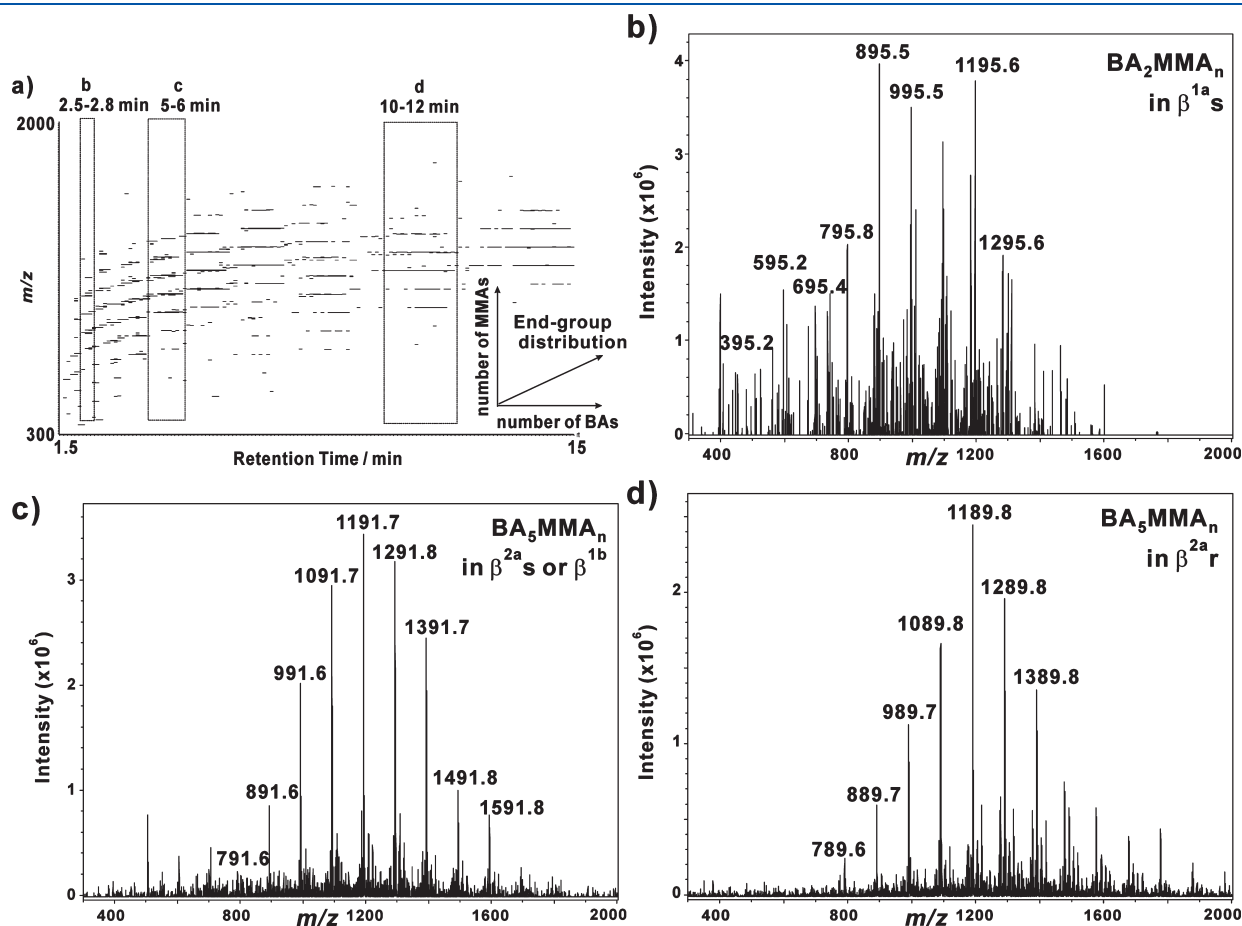


**Figure 6.** (a) Isocratic elution LC-MS data obtained on IT MS showing log abundance of the P(MMA-*r*-BA) with sodium adduct ions (data point weight) in a coordinate system of  $m/z$  (as  $y$ -axis) versus retention time (as  $x$ -axis). The corresponding average mass spectra of P(MMA-*r*-BA) in different retention time windows: (b) 2.5–2.8 min, (c) 5–6 min, and (d) 10–12 min.

the end-group functionality (polarity) and the number of BA units. The MMA effect on elution is ultimately minimized in this condition. The observed ranges of number of MMA and BA are 0–18 and 0–14, respectively. One drawback of this experiment is the possible ion suppression due to the elution of a large amount of different molecules in a relatively short retention time window.

A different approach to analyze the copolymer system would be to find the near-critical condition for the BA fraction.<sup>22</sup> Contrary to the condition applied in this study, a near-critical condition for BA will minimize the influence of BA on LC elution. The copolymer elution would then behave as influenced by end-group functionality and number of MMA units. This will be highly complementary to the study in this report.

## CONCLUSIONS

The results obtained with both gradient and isocratic elution conditions online coupled with MS show that the relatively reactive solvent, butyl acetate in this case, influenced the compositions of PMMA and P(MMA-*r*-BA). The effect of  $\beta$ -scission during polymerization on the copolymer composition is dominant. All four series found in the copolymer resulted from  $\beta$ -scission. Its effect on PMMA homopolymer composition is minor but difficult to evaluate accurately since the corresponding mass peaks have relatively low intensities. Isobaric materials with subtle structural differences (end-group) are easily identified by applying different isolation windows in high-resolution and high-accuracy MS<sup>2</sup> experiment when an LC-MS experiment alone is not sufficient for such analysis. Although the structures could still be assigned, application of gradient elution LC-MS to the complex copolymer system presented more difficulties to fully analyze all the end-groups of the peaks with relatively low intensity, such as peaks from series  $\beta^{1a}$ s. A near-critical condition achieved on PMMA using isocratic elution LC-MS facilitates separation of PMMA based on end-group functionality. Application of the same isocratic elution condition to the P(MMA-*r*-BA) polymer reduced the effect of the MMA fraction on elution time to almost none and therefore allows identification of copolymer with different end-groups in a shorter analysis time compared to gradient elution LC-MS. The methodology is generically applicable to PMMA copolymers and can (in a modified form) be extended to other copolymer systems as well.

## ASSOCIATED CONTENT

**S Supporting Information.** An example of identification of elemental compositions of the end-groups appearing in the PMMA using a linear regression method, and structure illustration of the end-groups mentioned in Table 2. This material is available free of charge via the Internet at <http://pubs.acs.org>.

## AUTHOR INFORMATION

### Corresponding Author

\*E-mail: [oscar.vandenbrink@akzonobel.com](mailto:oscar.vandenbrink@akzonobel.com).

## ACKNOWLEDGMENT

This work was funded by a European Community in the framework of the Marie Curie Early Stage Training Program POLY-MS (MEST-CT-2005-021029). J.S. acknowledges AkzoNobel for financial support. Leo G. J. van der Ven, Marco

Koenraadt, and Ber Yebio from AkzoNobel Car Refinishes, Sassenheim, The Netherlands, are acknowledged for the preparation of the acrylic resins. We thank B. Kruisselbrink for the GPC analysis. We also acknowledge A. Buijtenhuijs and Dr. A. T. Jackson for useful discussions.

## REFERENCES

- (1) Percec, V. *Chem. Rev.* **2009**, *109*, 4961–4962.
- (2) Kobayashi, S.; Makino, A. *Chem. Rev.* **2009**, *109*, 5288–5353.
- (3) Barbey, R.; Lavanant, L.; Paripovic, D.; Schuwer, N.; Sugnaux, C.; Tugulu, S.; Klok, H.-A. *Chem. Rev.* **2009**, *109*, 5437–5527.
- (4) Braunecker, W. A.; Matyjaszewski, K. *Prog. Polym. Sci.* **2007**, *32*, 93–146.
- (5) Georges, M. K.; Veregin, R. P. N.; Kazmaier, P. M.; Hamer, G. K. *Macromolecules* **1993**, *26*, 2987–2988.
- (6) Matyjaszewski, K.; Xia, J. *Chem. Rev.* **2001**, *101*, 2921–2990.
- (7) Moad, G.; Rizzardo, E.; Thang, S. H. *Polymer* **2008**, *49*, 1079–1131.
- (8) Buback, M.; Frauendorf, H.; Gunzler, F.; Vana, P. *J. Polym. Sci., Part A: Polym. Chem.* **2007**, *45*, 2453–2467.
- (9) Song, J.; van Velde, J. W.; Vertommen, L. L. T.; van der Ven, L. G. J.; Heeren, R. M. A.; van den Brink, O. F. *Macromolecules* **2010**, *43*, 7082–7089.
- (10) Subrahmanyam, B.; Baruah, S. D.; Rahman, M.; Baruah, J. N.; Dass, N. N. *J. Polym. Sci., Part A: Polym. Chem.* **1992**, *30*, 2531–2549.
- (11) Brandrup, J.; Immergut, E. H.; Grulke, E. A.; Abe, A.; Bloch, D. R. *Polymer Handbook*, 4th ed.; John Wiley & Sons: New York, 1999; p II/104.
- (12) van Herk, A. M. *Macromol. Rapid Commun.* **2001**, *22*, 687–689.
- (13) Matyjaszewski, K.; Davis, T. P. *Handbook of Radical Polymerization*; Wiley-Interscience: New York, 2003.
- (14) Quan, C.; Soroush, M.; Grady, M. C.; Hansen, J. E.; Simonsick, W. J. *Macromolecules* **2005**, *38*, 7619–7628.
- (15) Junkers, T.; Koo, S. P. S.; Davis, T. P.; Stenzel, M. H.; Barner-Kowollik, C. *Macromolecules* **2007**, *40*, 8906–8912.
- (16) Junkers, T.; Barner-Kowollik, C. *J. Polym. Sci., Part A: Polym. Chem.* **2008**, *46*, 7585–7605.
- (17) Jovanovic, R.; Dubé, M. A. *J. Appl. Polym. Sci.* **2001**, *82*, 2958–2977.
- (18) Jovanovic, R.; Dubé, M. A. *J. Appl. Polym. Sci.* **2004**, *94*, 871–876.
- (19) McKenna, T. F.; Villanueva, A.; Santos, A. M. *J. Polym. Sci., Part A: Polym. Chem.* **1999**, *37*, 571–588.
- (20) Falkenhagen, J.; Much, H.; Stauf, W.; Muller, A. H. E. *Macromolecules* **2000**, *33*, 3687–3693.
- (21) Jiang, X.; Lima, V.; Schoenmakers, P. J. *J. Chromatogr., A* **2003**, *1018*, 19–27.
- (22) Jiang, X.; Schoenmakers, P. J.; Lou, X.; Lima, V.; van Dongen, J. L. J.; Brokken-Zijp, J. *J. Chromatogr., A* **2004**, *1055*, 123–133.
- (23) Whitehouse, C. M.; Dreyer, R. N.; Yamashita, M.; Fenn, J. B. *Anal. Chem.* **1985**, *57*, 675–679.
- (24) Fenn, J. B.; Mann, M.; Meng, C. K.; Wong, S. F.; Whitehouse, C. M. *Science* **1989**, *246*, 64–71.
- (25) Crecelius, A. C.; Baumgaertel, A.; Schubert, U. S. *J. Mass Spectrom.* **2009**, *44*, 1277–1286.
- (26) Gruendling, T.; Weidner, S.; Falkenhagen, J.; Barner-Kowollik, C. *Polym. Chem.* **2010**, *1*, 599–617.
- (27) Montaudo, M. S.; Montaudo, G. *Macromolecules* **1999**, *32*, 7015–7022.
- (28) Gruendling, T.; Guilhaus, M.; Barner-Kowollik, C. *Macromolecules* **2009**, *42*, 6366–6374.
- (29) Falkenhagen, J.; Weidner, S. *Anal. Chem.* **2008**, *81*, 282–287.
- (30) Girod, M.; Phan, T. N. T.; Charles, L. *Rapid Commun. Mass Spectrom.* **2008**, *22*, 3767–3775.
- (31) Stülten, D.; Lamshöft, M.; Zühlke, S.; Spittler, M. *J. Pharm. Biomed. Anal.* **2008**, *47*, 371–376.



- (32) Song, J.; Grün, C. H.; Heeren, R. M. A.; Janssen, H-G.; van den Brink, O. F. *Angew. Chem. Int. Ed.* **2010**, *49*, 10168–10171.
- (33) Trimpin, S.; Plasencia, M.; Isailovic, D.; Clemmer, D. E. *Anal. Chem.* **2007**, *79*, 7965–7974.
- (34) Belov, M. E.; Rakov, V. S.; Nikolaev, E. N.; Goshe, M. B.; Anderson, G. A.; Smith, R. D. *Rapid Commun. Mass Spectrom.* **2003**, *17*, 627–636.
- (35) Staal, W. J. Gradient Polymer Elution Chromatography - A qualitative study on the prediction of retention times using could-points and solubility parameters. Ph.D. Thesis, Technische Universiteit Eindhoven, 1996.
- (36) van Rooij, G. J.; Duursma, M. C.; Heeren, R. M. A.; Boon, J. J.; de Koster, C. G. *J. Am. Soc. Mass Spectrom.* **1996**, *7*, 449–457.
- (37) Cools, P. J. C. H.; van Herk, A. M.; German, A. L.; Staal, W. *J. Liq. Chromatogr.* **1994**, *17*, 3133–3143.
- (38) Philipsen, H. J. A.; Klumperman, B.; van Herk, A. M.; German, A. L. *J. Chromatogr., A* **1996**, *727*, 13–25.